Supplement of Clim. Past, 15, 927–942, 2019
https://doi.org/10.5194/cp-15-927-2019-supplement

Climate of the Past
Open Access
EGU

Supplement of

Holocene hydrography evolution in the Alboran Sea: a multi-record and multi-proxy comparison

Albert Català et al.

Correspondence to: Albert Català (al_catala@ub.edu)

Table S1: Core location and information included in the discussion.

Table S2: Radiocarbon ^{14}C AMS dates from the ALB-2 core. Dates are calibrated with the MARINE13 calibration curves (Reimer, et al., 2013)

Figure S3: ALB-2 age-depth model based on Bayesian accumulations simulations (Blaauw and Christen, 2011). (a) The three upper plots show the stable MCMC run achieved (left), the prior (green line) and posterior (grey) distributions of the accumulation rates (middle), and the prior (green line) and posterior (grey) distributions of the memory (right). The main graph shows (c) the age-depth model with its errors. Yellow dots, correspond to those tie-points (most recent, the recovering year of the core, and the last pone is product of the correlation with the well-expressed event in (b) MD99-2343 record. (d) Show the location of these dates on the ALB-2 $\delta^{18}O$ ‰ (VPDB). (e) Show the accumulation rates in (cm/kyr).

Table S4: Radiocarbon ^{14}C AMS dates from the MD99-2343 core. Dates are calibrated with the MARINE13 calibration curves (Reimer, et al., 2013)

Figure S5: MD99-2343 age-depth improved from the original published by Frigola et al. (2007). The age model is based on Bayesian accumulations simulations (Blaauw and Christen, 2011). (a) The three upper plots show the stable MCMC run achieved (left), the prior (green line) and posterior (grey) distributions of the accumulation rates (middle), and the prior (green line) and posterior (grey) distributions of the memory (right). The main graph shows (c) the age-depth model with its errors. Yellow dots, correspond to those tie-points (most recent, the recovering year of the core, and the other two points are product of the correlation with the well-expressed event in (b) MD95-2043 record. (d) Show the location of these dates on the MD99-2343 $\delta^{18}O$ ‰ (VPDB). (e) Show the accumulation rates in (cm/kyr).

Figure S6: Comparison for all ALB-2 data obtained between the G. bulloides Mg/Ca ratios with (a) Al/Ca and (b) Mn/Ca ratios (Pena et al., 2005). In both plots red dots are those samples that were removed to avoid possibles interferences in Mg/Ca – SST.

Section 7: The theoretical carbonate $\delta^{18}O$ signal in VPDB (‰) has been estimated for the upper 100 meters in the studied area and during different seasons after: (1) Estimating the present local $\delta^{18}O$ and salinity relationship in base to the Alboran Sea data from Pierre (1999): $S(psu)=0.995* \delta^{18}O_{sw}-35.668$. (2) This equation has been applied to obtain the theoretical $\delta^{18}O_{sw}$ for the upper 100 mwd in the studied area at different seasons in base to the salinity data from site 503737B, obtained from WOA13 0.25deg, and integrates water measurements from 1955 to 2012. (3) This estimated $\delta^{18}O_{sw}$ has been transferred to carbonate $\delta^{18}O$ through the temperature equation form Shackleton, 1974: $T(°C)=16.9-4(\delta_c-\delta_{sw})$ and after the standard conversion $\delta_{sw}(VPDB)=0.99973* \delta_{sw}(SMOW)-0.27$. Temperature data was obtained from site 503737B, (WOA13 0.25deg measured during the years 1955–2012).

REFERENCES

Blaauw, M. and Christen, J. A.: Bacon manual – v2.2, , 1–11, 2011.

Frigola, J., Moreno, A., Cacho, I., Canals, M., Sierro, F. J., Flores, J. A., Grimalt, J. O., Hodell, D. A. and Curtis, J. H.: Holocene climate variability in the western Mediterranean region from a deepwater sediment record, Paleoceanography, 22, 2209, doi:10.1029/2006PA001307, 2007.

Frigola, J., Moreno, A., Cacho, I., Canals, M., Sierro, F. J., Flores, J. A. and Grimalt, J. O.: Evidence of abrupt changes in Western Mediterranean Deep Water circulation during the last 50 kyr: A high-resolution marine record from the Balearic Sea, Quat. Int., 181(1), 88–104, doi:10.1016/j.quaint.2007.06.016, 2008.

Pena, L. D., Calvo, E., Cacho, I., Eggins, S. and Pelejero, C.: Identification and removal of Mn-Mg-rich contaminant phases on foraminiferal tests: Implications for Mg/Ca past temperature reconstructions, Geochemistry, Geophys. Geosystems, 6(9), doi:10.1029/2005GC000930, 2005.

Pierre, C.: The oxygen and carbon isotope distribution in the Mediterranean water masses, Mar. Geol., 153, 41–55, 1999.

Reimer, P. J., Bard, E., Bayliss, A., Beck, J. W., Blackwell, P. G., Bronk, C., Caitlin, R., Hai, E. B., Edwards, R Lawrence Friedrich, M., Grootes, P. M., Guilderson, T. P., Haflidason, H., Hajdas, I., Hatté, C., Heaton, T. J., Hoffmann, D. L., Hogg, A. G., Hughen, K. A., Kaiser, K. F., Kromer, B., Manning, S. W., Niu, M., Reimer, R. W., Richards, D. A., Scott, E. M., Southon, J. R., Staff, R. A., Turney, C. S. M. and van der Plicht, J.: INTCAL13 AND MARINE13 RADIOCARBON AGE CALIBRATION CURVES 0–50,000 YEARS CAL BP, Radiocarbon, 55(4), 1869–1887, doi:https://doi.org/10.2458/azu_js_rc.55.16947, 2013.

Shackleton, N.: Attainment of isotopic equilibrium between ocean water and the benthonic foraminifera genus Uvigerina: isotopic changes in the ocean during the last glacial, CNRS, Colloq. Int., 219, 203–209, 1974

World Ocean Atlas 2013 Product Documentation. T Boyer, Ed.; A. Mishonov, Technical Ed.; 14 pp.

Supplementari Figure
Table S1

Core	Location		Depth (mwd)	References
	Latitude	Longitude		
HER-GC-ALB-2	36°0'44.80" N	4°16'24.38" W	1313	Català *et al*., 2019
ODP976	36°12' N	4°18' W	1108	Jiménez-Amat and Zahn, 2015
MD95-2043	36°8'598" N	2°37'269" W	1841	Cacho *et al*., 1999
MD99-2343	40°29.84' N	4°01.69' E	2391	Frigola *et al*., 2007

Supplementari Figure
Table S2

Depth, cm	Specie	Age ^{14}C years BP	2σ error	Calendar Years
0	Tie Point (Recovered core year)	-	-	-56
10	*G. inflata*	725	25	407
15	*G. inflata*	1334	29	856.5
26	*G. inflata*	2097	26	1668
36	*G. inflata*	2688	26	2355.3
62	*G. inflata*	3778	28	3706.8
83	*G. inflata*	4538	27	4703.1
112	*G. inflata*	5370	30	5866
114	*G. inflata*	5773	31	5996.9
131	*G.inflata*	6200	90	6709.5
153	*G.inflata*	7170	85	7686.8
184	*G. inflata, N. pachyderma, G. bulloides*	8814	41	9192.1
209	*G. inflata, N. pachyderma*	9190	35	10094.2
231	*G. inflata, N. pachyderma*	10084	45	11094
265	*G. inflata, N. pachyderma, G. bulloides*	11194	42	12699.8
314	Tie Point (MD95-2043)	-	-	14610

Supplementari Figure
Figure S3

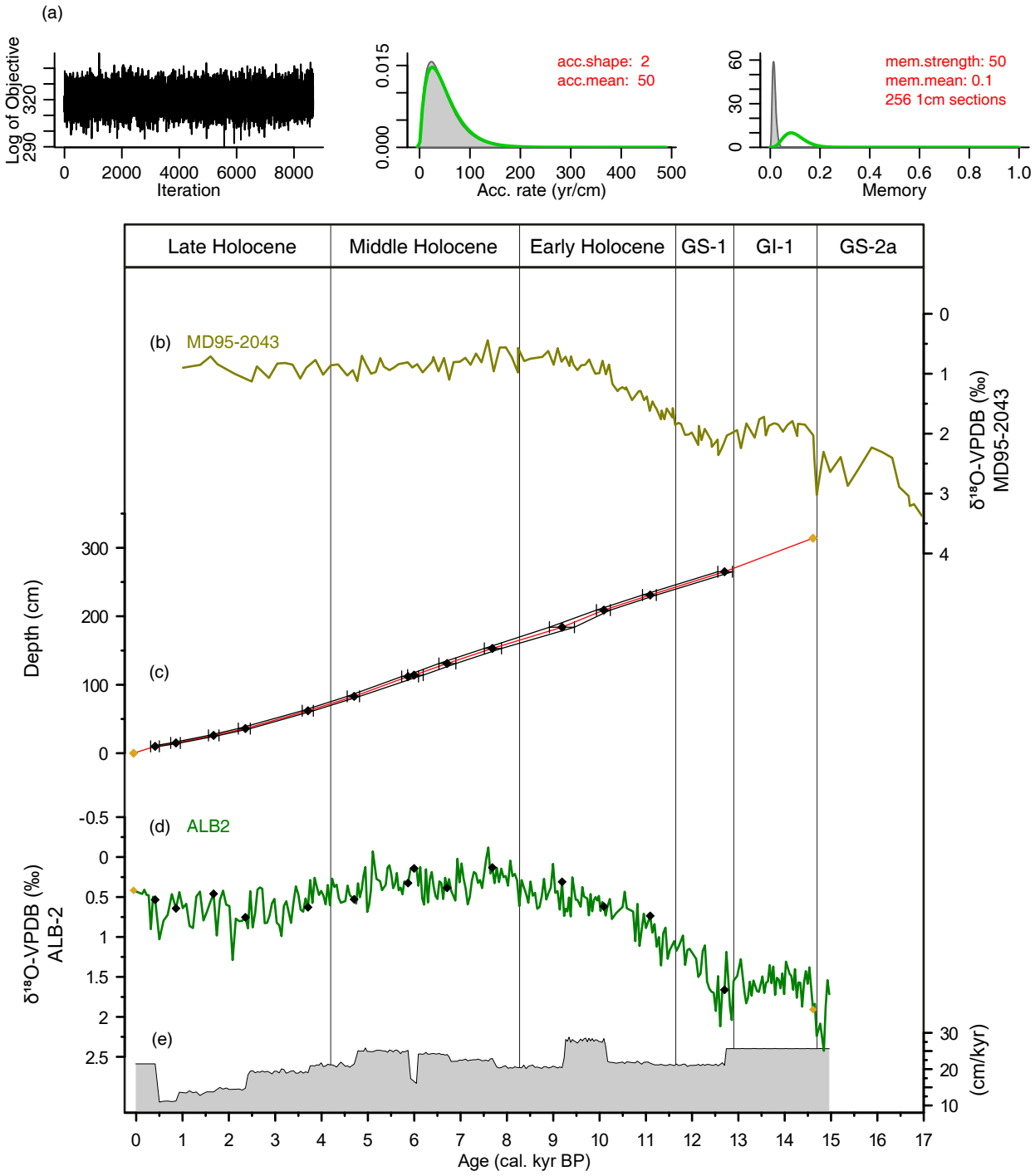

Supplementari Figure
Table S4

Depth, cm	Isotop Event/Radiocarbon Samples	Age ^{14}C years BP	2σ error	Calendar Years
0	Tie Point (Recovered core year)			-49
28	^{14}C AMS	790	89	436
42	^{14}C AMS	1090	61	680.3
54	^{14}C AMS	1520	90	1093.6
88	^{14}C AMS	3110	94.5	2612.4
118	^{14}C AMS	3390	142.5	3283.2
144	^{14}C AMS	3880	111	3887.9
184	^{14}C AMS	4850	128.5	5164.5
208	^{14}C AMS	5720	388.5	6009
238	^{14}C AMS	6210	135.5	6624.8
274	^{14}C AMS	6720	74	7314.6
296	^{14}C AMS	7580	107	7990.4
308	^{14}C AMS	7700	121	8266.4
312	^{14}C AMS	7660	85.5	8427.7
334	^{14}C AMS	8750	106	9411.1
364	^{14}C AMS	9890	180	10793
398	^{14}C AMS	10650	207	11978.1
418	^{14}C AMS	11200	116	12670.4
485	Tie Point - Base of GI-1			14622.4
534	Tie Point - Top Anomaly GS-2a			15373.2
568	^{14}C AMS	14550	344	16163.3
604	^{14}C AMS	13850	345	16980.9

Supplementari Figure
Figure S5

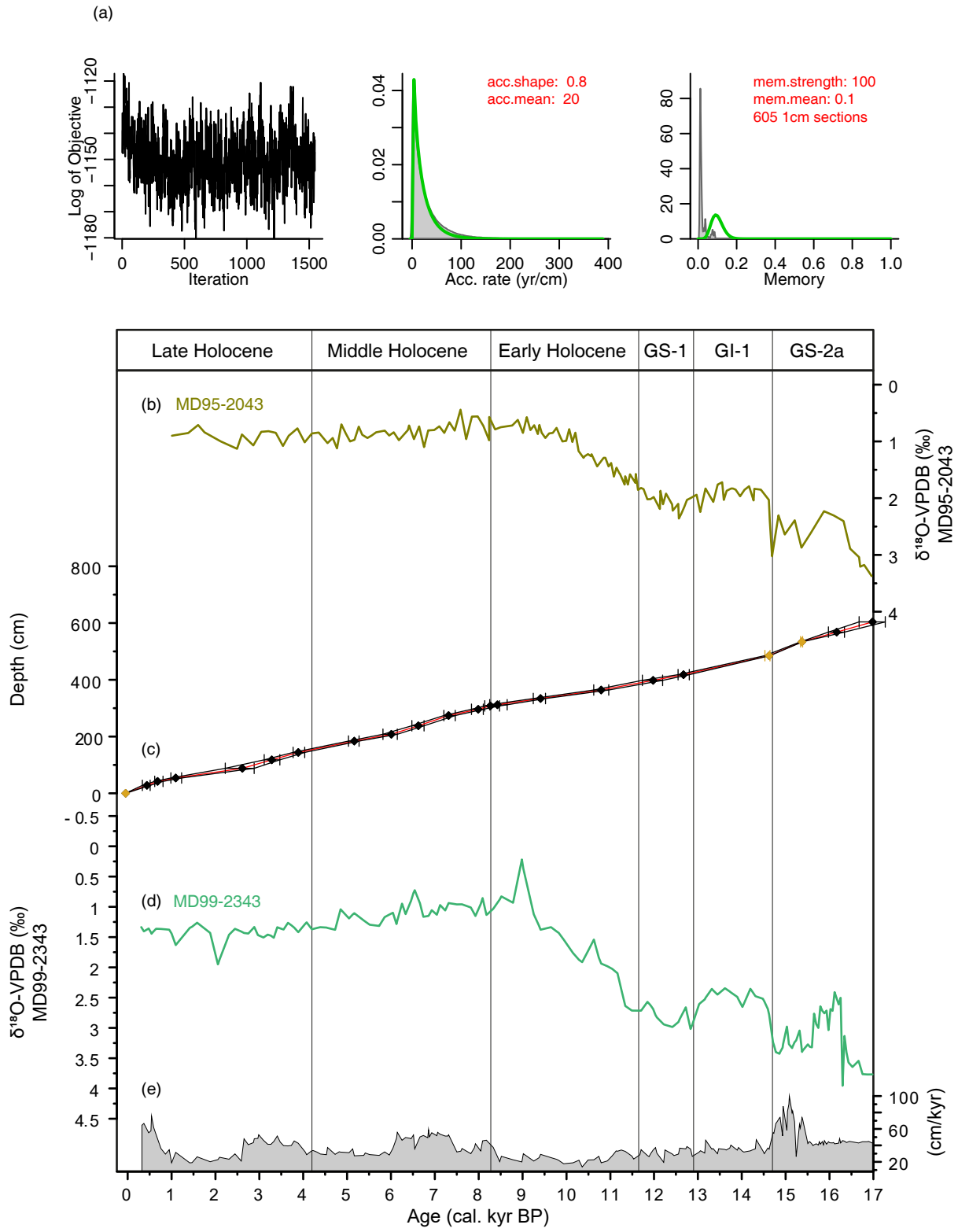

Supplementari Figure
Figure S6